Biomass Conversion and Biorefinery (2026) 16:135
https://doi.org/10.1007/s13399-025-06936-4

ORIGINAL ARTICLE

Utilization of gold-loaded ironbark biochar-based catalyst for catalytic upgrading of spent coffee grounds: reaction kinetics, products distribution, and mechanism

Mahmuda Akter Mele[1] · Ravinder Kumar[1] · Ioan Sanislav[1] · Elsa Antunes[1]

Received: 11 May 2025 / Revised: 3 December 2025 / Accepted: 13 December 2025

Abstract
To reduce dependence on fossil fuels and limit environmental impacts, converting abundant and low-cost lignocellulosic biomass into renewable energy products is essential. While biomass-derived biochar is widely used in environmental and agricultural applications, its role as a catalyst or catalytic support has received far less attention. In this study, we develop a novel biochar-based catalyst and demonstrate its effectiveness in the catalytic pyrolysis of spent coffee grounds (SCG), leading to enhanced production of valuable hydrocarbons and phenols. This work reveals a new and underexplored application of biochar in sustainable energy and chemical generation. The adsorption method was adopted for the preparation of gold nanoparticles (AuNPs) loaded into ironbark biochar (IBBC) catalysts. The characterization by BET, XRD, FTIR, SEM-EDS findings confirmed the successful preparation of AuNPs-IBBC catalyst. SCG biomass, without-metal catalyst showed the lowest hydrocarbon production. However, incorporating the AuNPs-IBBC into the process led to an increase in the production of aromatics, as well as aliphatic hydrocarbons. The biochar surface functionalities coupled with gold increased the aromatics selectivity two-fold (from 4.5 to 9.9%) and phenols (from 2.4 to 5.5%) with the IBBC-BC1 catalyst. At 750 °C pyrolysis temperature with the BC1 catalyst, hydrocarbon production was the highest compared to other catalysts. The BC1 catalyst favored C4–C11 hydrocarbons with a selectivity of 6%. The BC1 catalyst has demonstrated an enhanced pore volume of 0.089 cm^3/g, accompanied by an average pore diameter of 3.182 nm. TGA results showed significant weight reduction rates and increased thermal degradation rates after catalytic pyrolysis of SCG. Therefore, it could be suggested that gold-loaded biochar catalyst can upgrades the SCG biomass to produce value-added chemicals.

Keywords Biochar catalyst · Gold nanoparticles · Catalytic pyrolysis · Bio-oil · Hydrocarbons

Highlights
- A catalyst of biochar-Au nanoparticles was successfully synthesized.
- The catalyst showed improved textural properties compared to the control biochar.
- TGA confirmed enhanced weight reduction rates with Au-biochar catalyst.
- Au-biochar catalyst showed the highest production of hydrocarbons and phenols.
- 750 °C was favourable to achieve the highest quantity of hydrocarbons.

1 Introduction

The increased utilization of fossil fuels has given rise to significant concerns regarding energy security and pollution of the environment, which in turn accelerates the search for renewable energy sources [1]. Biomass, a prominent renewable energy source, has come into focus as a prospective candidate to mitigate these adverse effects [1]. Biomass plays a crucial role in meeting approximately 10% of the earth's energy demands [2]. Moreover, the potentiality of biomass as a renewable power source is enormous, particularly when harnessed through environmentally friendly methods such as thermochemical pathways like pyrolysis or gasification. The pyrolysis method requires the breaking of biomass to produce bio-oil, biochar, and syngas [2]. Bio-oil

✉ Elsa Antunes
elsa.antunes1@jcu.edu.au

[1] College of Science and Engineering, James Cook University, Townsville, QLD 4811, Australia

Published online: 07 February 2026

produced from pyrolysis has a valuable fuel for many uses and also as a hydrocarbon feedstock that could be easily added to bio-refineries [3] The bio-oil has a higher heating value (HHV) of 17.23 MJ/kg which is less than traditional fuel [4]. This is because it has oxygen-containing molecules like linoleic acid, palmitic acid, esters, and ketones, which make up about 59.5 wt% of its total weight. Consequently, a significant amount of research focuses on enhancing the hydrocarbons output in bio-oil to enhance its quality and address these issues [5]. Catalysts can transform oxygen-containing molecules with low energy into aromatic hydrocarbons with high energy, thus increasing the calorific heating value of bio-oil [4].

Catalytic pyrolysis (CP) is considered a method for the modification of biomass into liquid bio-oil due to its simplicity, efficiency, and cost-effectiveness. Catalysts have been used to increase the effectiveness of the pyrolysis technique. For example, catalytic reactions such as cracking, aromatization, deoxygenation, and dehydrogenation, can be activated by the addition of a suitable catalyst, which makes possible the production of upgraded chemicals [6]. For instance, pine wood sawdust has been used for catalytic upgrading of biomass [7]. Several biochar catalysts were synthesized by altering biochar with various metal loadings (Zn, Fe) and subjecting them to activation by CO_2, and H_2O. The CP of pine wood sawdust generates high-quality bio-oil which demonstrated significant deoxygenation capacity for ketones and acids in bio-oil and efficiently transformed lignin-derived chemicals into hydrocarbons and phenols.

Another study emphasized the influence of biochar catalysts on the catalytic pyrolysis of pine needle biomass [8]. The existence of surface acidic functions such as H_3PO_4, $ZnCl_2$, and NaOH with metallic site Ni with biochar enhanced the selectivity for aromatics. Likewise, aliphatics were increased to 9.61%, 10.12%, and 11.68% utilizing Ni/BC-$ZnCl_2$, Ni/BC-H_3PO_4, and Ni/BC-NaOH, respectively. Moreover, the presence of catalysts in the process of CP has gained consideration to enhance the yield of hydrocarbon compounds in bio-oil [9]. The CP of biomass has extensively used various catalysts, including hierarchical zeolites [10], microporous zeolites [11], mesoporous materials, and metal oxides [12], to enhance the production of aromatic hydrocarbons. Phenolic products with a high degree of purity have the potential to be subjected to established standards for various applications, including as cosmetic ingredients, food additives, dietary supplements, and pharmaceuticals [13]. In addition, phenol is used extensively in the production of many different compounds, including bisphenol A, caprolactam, phenol resins, adipic acid, and alkylphenols, making it an essential industrial chemical intermediate [14]. Moreover, phenol can be generated by the process of biomass catalytic pyrolysis using effective catalysts, including acids, bases, and carbonates such as sodium hydroxide (NaOH), and sodium carbonate ($NaCO_3$) potassium hydroxide (KOH), and activated carbon catalyst [14].

Despite extensive research on biochar such as soil enhancement, water purification, adsorbent, and the production of activated carbon due to their tunable properties. Biochar, an environmentally sustainable alternative, can also be used as a catalyst or catalytic agent. The surface structure, surface area, and surface functional groups on the biochar are critical factors when utilizing biochar as catalysts [15]. In recent times, there has been progress in the development of catalysts supported by biochar/engineered biochar for various applications such as biodiesel production [16], catalytic esterification [17], biogas reforming [18], and biomass hydrolysis [19]. The usage of catalysts for biomass upgrading such as zeolites and mesoporous silica, as discussed before, is costly due to extensive purification methods, leading to higher expenses and adverse effects on the environment. Therefore, a low-cost and renewable catalyst is necessary. Nevertheless, there has been a lack of research investigating the use of biochar catalysts in upgrading biomass. For instance, N-doped bamboo waste [20], microalgae/palm kernel shell [21], pinewood sawdust with modified biochar catalyst [7], Ni-functionalized activated biochar catalysts [8] have been employed recently for biomass upgrading. Currently, there is not enough demonstrated research on the utilization of biochar catalysts by CP of biomass for the production of high-quality biofuel.

Recently, discarded coffee grounds (SCG) have attracted attention as a prospective feedstock for thermochemical conversion in the context of CP. The coffee intake in worldwide ended up at 9.9 megatons (Mt) which makes it more popular than any other drink in 2021 [22]. Spent coffee grounds consist of common residential garbage that is typically disposed of via landfill or incineration [22]. However, discarding SCG by these processes creates challenges because of the considerable oxygen demand during decomposition and the possibility of releasing hazardous substances, including residual tannin, caffeine, and polyphenol [1]. The utilization of renewable bio-based materials will enhance sustainability by minimizing waste, landfills, and harmful emissions, resulting in a greener and cleaner environment [23]. However, considerable research has been done on the utilization of spent coffee grounds (SCG) in various sectors such as the production of biofuels/biodiesel [24], bioethanol [25], bio-hydrogen generation [26], adsorbent [27] and as soil amendment [28]. With its fuel and combustion properties, SCG-biochar shows great promise as an efficient biofuel for energy generation [29]. Recently, researchers have shown interest in producing biofuel by catalytic upgrading, such as marine biofuels [30], bioaromatics [31], and hydrocarbons [4]. However, CP of SCG biomass

using gold-loaded biochar has not been explored yet. Therefore, in this research, a novel approach has been taken for the CP of SCG biomass using biochar as the catalyst. In our previous studies [32], preliminary catalytic pyrolysis of IB sawdust biomass with gold-loaded IBBC catalyst has been effectively conducted, resulting in the production of phenolic compounds, and hydrocarbons in the bio-oil (supplementary information). The primary objective of this study was synthesizing gold-doped biochar catalysts from IB biomass using different concentration of gold (100, 200, and 300 mg/L). The prepared biochar catalysts were thoroughly characterized using various physicochemical techniques. Further, the catalysts were tested for the production valuable chemical products in CP of SCG biomass. Various parameters such as pyrolysis temperatures (450–750 °C), catalyst to biomass ratios (like 0:1, 1:1, 2:1, and 1:2) were analyzed to investigate their effect on chemical products distribution, especially, types of hydrocarbons. Finally, a possible mechanism of chemical products formation on gold-biochar catalyst was presented.

2 Materials and methods

2.1 Materials

Ironbark was collected from a nearby shop in Queensland's Townsville city. Gold chloride was purchased from Sigma-Aldrich. SCG biomass was collected from a barista coffee shop at James Cook University Townsville campus. To remove the moisture, SCG was dried overnight at 105 °C in an oven, and after fine powder was prepared by mechanical grinder from the James Cook University analytical center.

2.2 Production of biochar

The pyrolysis of ironbark sawdust was conducted with a nitrogen atmosphere utilizing a permanent bed reactor and a glass furnace (tube) as performed in previous research [32]. Approximately 5 to 10 g of IB was placed in a quartz holder and set up in a furnace for pyrolysis at 500 °C. The process was conducted with a residence time of 2 h and a heating rate of 10 °C/min. After the experiment, the biochar was weighed, crushed, collected, and stored in an airtight container.

2.3 Synthesis of gold nanoparticles ironbark Biochar catalyst (AuNPs-IBBC)

2.3.1 Adsorption experiment of IB biochar

Gold nanoparticles (AuNPs) loaded biochar catalyst was synthesized based on the previous work [32]. Ironbark biochar with no gold is considered as IBBC-BC0. In addition, gold with 100 (IBBC-BC1), 200 (IBBC-BC2), and 300 (IBBC-BC3) mg/L concentration of liquid solutions mixture were prepared by dissolving accurately weighted gold chloride with double-distilled water. For 100 and 200 mg/L concentration the biochar amount was taken 0.2 g. On the other hand, 300 mg/L, 0.1 g biochar was selected following the previous experimental results. Firstly, 500 ml volume of solution was used to conduct the gold adsorption experiment at room temperature (24º C) with stirred rotational speed of 440 rpm. After 23 h, the biochar loaded with AuNPs was collected by vacuum filter using a Buchner flask as well as with a Buchner funnel. After samples were kept in the oven at 80 °C and the next day collected the dried gold-loaded biochar catalyst.

After adsorption, around 20 mL of gold mixture solution was taken by a syringe and filtered by utilizing a 0.22 µm (membrane), and then the supernatant was examined by inductively coupled plasma-atomic emission spectroscopy (ICP-AES). The gold concentration in the solution was measured using ICP-AES before and after adsorption.

2.3.2 Catalyst characterization

Brunauer-Emmett-Teller (BET) method was used to examine the surface area of biochar samples. The nitrogen (N_2) adsorption-desorption isotherms of IB biochar were determined at 196 °C using a Micromeritics Tristar 3020 device. Prior to the analysis, biochar and after the adsorption experiment gold-loaded biochar catalysts were subjected to degassing at 300 °C for 6 h in inert conditions. The Barrett-Joyner-Halenda (BJH) isotherm was used to determine mesopore volume and diameter.

The crystallinity of biochar was determined using the X-ray diffraction (XRD) instrument before and after gold adsorption. The biochar catalyst was analyzed using a volume holder with a thinner slit of 0.2 mm. X-ray diffractometer (Bruker) was used, with the mode set to position the sensitive detector fast at continuous mode. The analysis was performed from 10 to 90° (degree), following XRD conditions, at a rate of 1 s per step with a step size increment of 0.02. In addition, the crystalline size of gold can be calculated from the XRD data using the Scherrer equation, which is utilized to find out the crystallite size of nanoparticles.

$$D = \frac{K\lambda}{B\cos\theta}$$

where, D (nm) signifies the mean dimension of the ordered (crystalline) domains, K represents the form factor often set at 0.9, and λ indicates the wavelength of the X-ray measured at 0.154 nm, β signifies the full width at half maximum

(FWHM) of diffraction peaks (in radians), and θ indicates the Bragg angle (in radians).

The morphological characteristics of biochar were determined using scanning electron microscopy (SEM) and energy dispersive X-ray spectroscopy (EDS). To conduct SEM-EDS examination, the IBBC was suspended in distilled water and then placed onto a silicon-coated wafer. The investigation was performed using an SEM (SU5000, OXFORD instrument, X-Max, Hitachi).

The Fourier Transform Infrared (FTIR) spectra of powdered biochar were confirmed using a Nicolet 6700 FTIR spectrometer using the Attenuated Total Reflectance (ATR) method employing a diamond crystal. With the cumulative scans amounted to 32, featuring a spectral resolution of 4 cm^{-1}. The Omnic Spectra software facilitated the understanding of certain data.

Thermal degradation of SCG and gold-loaded biochar catalysts was examined using a thermogravimetric (TGA) analyzer (NETZSCH STA 449F3) under a nitrogen atmosphere. The samples were placed in an alumina crucible (85µL) and heated from 26 to 1000 °C at a 30 °C/min heating rate.

2.3.3 Pyrolysis GC/MS method and design of experiment

The pyrolysis by GC/MS analysis was conducted using a CDS 6150 pyrolyzer (Pyroprobe). Throughout the pyrolysis experiment, the targeted pyrolysis temperature was maintained at four distinct levels: 450, 550, 650, and 750 °C. Each temperature setting was sustained for 27 min, while the heating rate remained constant at 10 °C/ms. The interface, GC transfer line, and valve oven were all maintained at a temperature of 300 °C. The by-products of pyrolysis were directed from the furnace tube (quartz) to a GC/MS (model 6890/5973 N, manufactured by Agilent) using helium [5]. The temperature of the GC/MS injector was set at 250 °C. The gas chromatography (GC) separation was conducted on an HP-5MS column with ultra-pure helium gas (99.99%) at a flow rate of 1.0 mL/min. The standard operating parameters for mass spectrometry (MS) typically involve an ionization energy which was 70 electron volts (eV) and the utilization of the mass-to-charge ratio (m/z) scanning mode within a range spanning from 25 to 550 atomic mass units (amu).

The Taguchi method was utilized in this initial stage to analyze the primary effects. The biochar catalyst with the highest concentration of hydrocarbon compounds was chosen for the subsequent stage. The Taguchi approach was utilized in Minitab 17 for statistical analysis to identify the primary effects of pyrolysis conditions on chemical distribution. Three variables (biochar catalyst, temperature, and catalyst: feedstock ratio) were selected at four levels, the sixteen runs of these factors were taken into consideration, as represented in Table 1. Figure **S1** presents the main effect plots for means and S/N ratio for these variables (see supplementary information), which could help to understand the overall process performance and robustness.

Table 1 Experimental design matrix: GC/MS catalytic pyrolysis of spent coffee ground biomass.

Run	Biochar Catalyst	Temperature	Catalyst: Feedstock ratio
1	BC 0	450	0:1
2	BC 0	550	1:1
3	BC 0	650	2:1
4	BC 0	750	1:2
5	BC1	450	1:1
6	BC1	550	0:1
7	BC1	650	1:2
8	BC1	750	2:1
9	BC2	450	2:1
10	BC2	550	1:2
11	BC2	650	0:1
12	BC2	750	1:1
13	BC3	450	1:2
14	BC3	550	2:1
15	BC3	650	1:1
16	BC3	750	0:1

IBBC-BC0; AuNPs-IBBC: BC1, AuNPs-IBBC: BC2 and AuNPs-IBBC: BC3

3 Characterization of Biochar and catalyst

The biochar catalyst demonstrated a well-developed porous structure; however, the effect of gold loading on the biochar varied significantly among different catalyst types. The BET specific surface area (S_{BET}) ranged from 167.54 to 225.70 m^2/g (BC1 > BC2 > BC3), with an average pore diameter of 3.05 to 3.18 nm, as indicated in Table 2, demonstrating the established microporous structure of the catalyst. Following gold adsorption, the total pore volume (V_{total}) of the gold-loaded biochar catalyst decreased from 0.167 to 0.064 cm^3/g, and the S_{BET} for BC0: 493.78 m^2/g to BC3: 167.545 m^2/g reduced likewise. A possible reason for the decrease in surface area could be the agglomeration of gold particles at higher concentrations on the biochar surface, which subsequently blocks the micropores and reduces N_2 gas adsorption. For instance, another study that has agreement with this result showed total pore volume of 0.167

Table 2 Textural properties of Biochar catalysts

Biochar catalyst	S_{BET} (m^2/g)	V_{total} (cm^3/g)	Average pore diameter, D (nm)
BC0	493.78	0.167	4.001
BC1	225.705	0.089	3.182
BC2	214.810	0.084	3.059
BC3	167.545	0.064	3.176

cm^3/g and S_{BET} of 322.38 m^2/g for sawdust biochar which has been used for the removal of perfluorooctanesulfonic acid [33]. However, BC1 exhibited the highest S_{BET} among the gold-loaded biochar catalysts. The specific surface area signifies numerous active sites for chemical interactions, producing biochar highly efficient for catalytic performance. Furthermore, the large S_{BET} would give numerous catalytic chemical transformation sites at the time of the CP method [34]. In addition, the pore size was sufficiently increased to permit the migration of intermediates into the pores, thereby promoting reactions at the active regions [35].

As shown in Fig. 1 BET graphs of IB catalysts (BC0, BC1, BC2, and BC3) exhibit mesoporous structural characteristics of a type IV isotherm according to IUPAC. A curved knee signifies the predicted sites for monolayer formation, while hysteresis points out the capillary precipitation in macro as well as micropores [36].

BC0 catalyst showed a higher surface area and pore volume than other catalysts, which were 493.78 m2/g and 0.167 cm3/g, respectively. However, a consistent decrease in surface area and pore volume was observed for other biochars (BC1, BC2 and BC3). For example, BC2 and BC3 showed surface areas of 214.81 and 167.54 m2/g whereas pore volumes for BC2 and BC3 were 0.084 and 0.064 cm3/g, respectively. This finding has shown similar results with microalgae biochar-based catalysts [21]. The mesoporous structure of all biochars could be quite advantageous since it can allow Au particles to enter and interact with the IBBC surface.

The crystalline structure of IBBC was assessed by XRD. Figure 2 displays the XRD pattern of IBBC before and after the gold adsorption, the results were compared with the standard XRD pattern of biochar (JCPDS card number. 50–0926) and AuNPs (JCPDS no: 00–004-0784) [37]. The XRD graph of IB biochar exhibited notable peaks at 2θ values of 22.8°, 29.4°, and 39.50°, indicating that the IBBC is mainly comprised of amorphous carbon in IBBC-BC0 [38]. The main characteristics of a prominent intensified band show that the primary surface linked to amorphous carbon was markedly decreased after the Au adsorption on all the biochar catalysts (BC1, BC2, and BC3), shown in Fig. 2 (a). It has been demonstrated that AuNPs were distinctly detected at 2θ values of 38.10° (111), 44.13° (200), 64.43° (220), and 77.32° (311) across all catalysts (BC1, BC2, and BC3) following gold adsorption onto biochar.

Table **S1** also showed the crystalline size of AuNPs after gold adsorption by IBBC using the Scherrer equation. BC3 showed the average 22.81 nm gold nanoparticles size whereas BC1 showed 22.35 nm. Interestingly, there is a significant difference among the biochar catalysts. For example, BC3 has the highest gold adsorption capacity so the nanoparticle sizes are larger for BC3 according to XRD, which was confirmed by Scherrer equation.

Figure 2(b) illustrates the results of the FTIR studies on IBBC with and without gold. FTIR was used to analyze the changes in chemical functional groups on biochar before and after gold loading. For example, aromatic and heteroaromatic compounds are validated by C-H wagging vibrations in the range of 800 to 600 cm^{-1} for BC0 which are sharper with gold (BC1, BC2, BC3) loadings. Additionally, the prominent peak near 1037 cm^{-1} in IBBC is ascribed to the stretching of the C-O functional group. The intensity of that peak is significantly higher in IBBC loaded with gold than in biochar without gold. BC0 and BC1, BC2, and BC also have intense vibrations at 1544 cm^{-1}. For example, wastewater sludge biochar prepared at 500 °C has also shown similar band associated with C-N-C bending vibrations at 1544 cm^{-1} [39]. Further, the bands at 1432 cm^{-1} correspond to CH_2 vibrations. The peaks about 1644 cm^{-1} belong to amide bonds, which are also present in all the samples [40]. All biochar and biochar catalysts showed two distinct peaks at around 3700 cm^{-1} and 3600 cm^{-1} corresponding to the vibrations of OH groups.

SEM and EDS were used to examine the macroscopic characteristics and Au adsorption on IBBC biochar. SEM was utilized to determine the shape and features of IBBC prior to and after Au adsorption. Figure 3 presents SEM pictures at different magnifications of IBBC, exhibiting its morphological and pore-size structural characteristics. The IBBC showed rigid, uneven surfaces marked by both irregular and regular roughness, as well as channels, small uniform particles, and flat areas. For instance, the result has been comparable [41, 42] to that recorded for modified eucalyptus bark biochar [43]. Figure 3 **(b)** depicts the morphology of IBBC, accompanied by the EDS images following gold the adsorption of IBBC from the liquid solution. The EDS pictures verified that the white marks are AuNPs and demonstrated the deposition of gold on the surface of IBBC. Moreover, carbon was primarily found in the IBBC, and the EDS elemental analysis revealed the presence of AuNPs in all three catalysts. Gold depositions in all three catalysts exceedingly roughly 84.87%, which had been attached on the surfaces of the biochar. The SEM micrographs of the biochar catalysts (Fig. S1) show that the biochar catalyst from BC1 displayed improved porosity, possessing a more advanced porous structure compared to those from BC2 and BC3. The depicted figure shows that the IBBC particles have an irregular morphology and implies the synthesis and deposition of gold nanoparticles on the biochar surface.

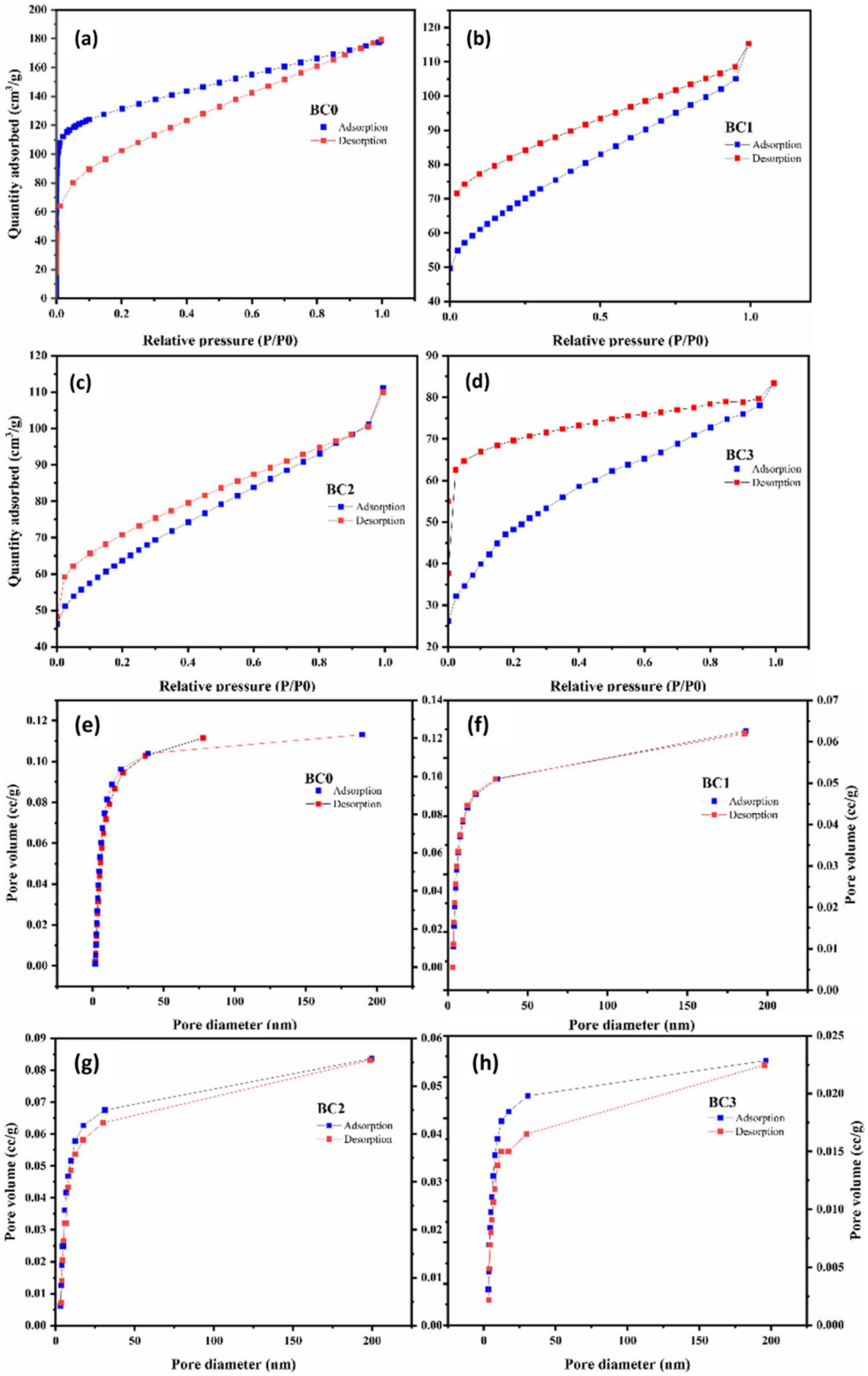

Fig. 1 Nitrogen adsorption-desorption isotherms (**a**-**d**) BET; pore diameter analysis by BJH (**e**-**h**) of IBBC catalyst IBBC-BC0, AuNPs-IBBC: BC1, AuNPs-IBBC: BC2 and AuNPs-IBBC: BC3

4 Pyrolysis kinetics: TGA/DTGA

The TGA and DTGA of non-catalytic and CP of SCG are shown in Fig. 4. Three phases can be identified in the thermal breakdown of SCGs. The initial phase, which takes place between 26 and 200 °C, is usually referred to as dehydration. At temperatures between 180 and 300 °C, hemicellulose breaks down into smaller molecules like sugars and furans.

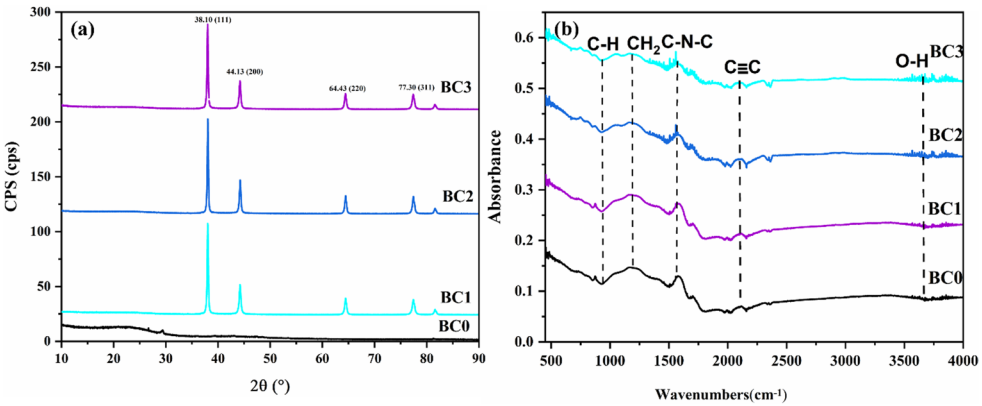

Fig. 2 (**a**) XRD of Gold loaded Ironbark biochar BC0: no gold, BC1: 100 mg/L, IB-BC2: 200 mg/L, IB-BC3: 300 mg/L gold catalyst; (**b**) FTIR of gold-loaded Ironbark biochar BC0: no gold, BC1: 100 mg/L, BC2: 200 mg/L, BC3: 300 mg/L gold catalyst

It then fully depolymerizes at temperatures until to 350 °C, producing volatile organic compounds, carbon monoxide, carbon dioxide, and other gases [44]. In SCGs, the percentage of cellulose can range from 30% to 40% [45]. Phenols, furans, aldehydes, acids, ketones, and gaseous products, including carbon monoxide, carbon dioxide, hydrogen, and methane, are among the complex combination of organic compounds that are formed as cellulose degrades, which begin from around 180 °C and are fully depolymerized by 400 °C [46]. Lignin makes up about 20–30% of SCGs [45]. A slight weight loss of 5.20 weight% was observed at this step, which is explained by the loss of other volatile organic molecules that are frequently present in biomass feedstocks, such as alcohols, ketones, and aldehydes.

However, the three stages of the catalytic pyrolysis of SCG utilizing gold-loaded IBBC catalysts have illustrated in the thermal decomposition profile in Fig. 4 (a). The first stage is similar to SCG without a catalyst. The second stage, known as devolatilization, takes place between 200 and 500 °C [45]. The main process for the breakdown of cellulose and other larger molecular weight components in SCG was the second stage, which lasted from 200 to 500 °C. SCG demonstrated the highest weight loss at 67.20% at 500 °C. These findings are consistent with a prior study [21] that found comparable weight reduction rates for SCG TGA analysis. However, at 500 °C, BC1 has shown the least amount of weight loss of 48.42%. At 200 and 500 °C, BC2 and BC3 catalysts showed the highest weight loss at 58.01% and 56.76%, respectively. This weight loss between 200 and 500 °C could be attributed to the degradation of complex macromolecular structure known as lignin into smaller molecules such as aldehydes, phenols, and aromatic chemicals [46]. Fatty acids, aldehydes, and chemicals containing nitrogen are produced when the proteins and lipids found in SCG break down between 200 and 500 °C [47].

The last phase, known as carbonization, takes place between 500 and 1000 °C. Weight loss of 4.40% was observed at this stage for SCG, which is explained by the creation of carbonaceous materials and the breakdown of residual organic components. Gold-loaded biochar catalysts enhance the generation of gases and coke by promoting the dehydrogenation process and raising the degree of ring-opening reaction at temperatures between 500 and 1000 °C. For instance, when compared to the other catalysts (BC1, BC2, and BC3), BC0 showed the highest solid content (8.52%). As a result, TGA measurements demonstrated that the catalysts successfully enhanced the SCG degradation. The DTGA graph, Fig. 4 (b), indicated that the highest degradation took place between at 301.9 to 304.1 °C whereas the thermal depolymerization of the SCG mostly was performed at 305 °C. The thermal degradation of SCG was 69.74% which was lower than with the gold-loaded biochar catalyst (ranging from 76.29% to 79%).

5 Results and discussions

5.1 Preliminary results

Chemical product distribution produced from catalytic pyrolysis of SCG biomass and AuNPs loadedIBBC mixture via Py-GC/MS are shown in Figure S2 (supplementary information). Initial results confirmed the gold-loaded biochar-based catalysts mainly promoted the formation of phenols and hydrocarbons. Then the AuNPs-IBBC biochar catalyst was designed to improve the hydrocarbon yield. Chemical products distribution at different temperatures without a catalyst are shown in Fig. 5. This figure is discussed in further sections of results and discussion.

5.2 Catalytic pyrolysis of spent coffee grounds by GC/MS

5.2.1 Effect of gold concentration

Figure 6 illustrates the changes in the primary chemical groups corresponding to different biochar catalyst loadings. When the SCG was tested at varying gold loading

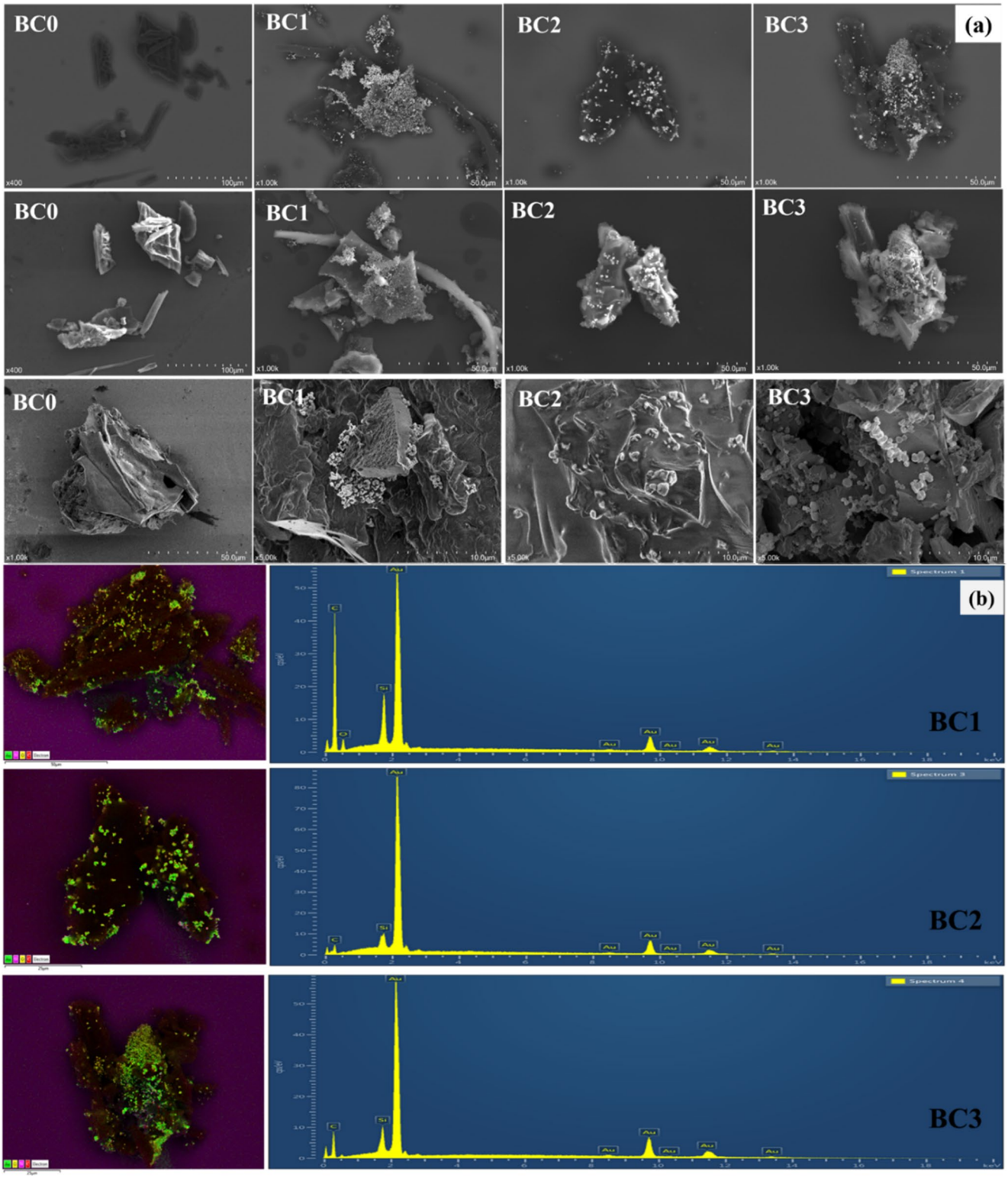

Fig. 3 (**a**) SEI, BEI and SEM images of gold loaded biochar catalyst where Ironbark biochar BC0: no gold (IBBC), BC1: 100 mg/L gold, BC2: 200 mg/L gold, BC3: 300 mg/L gold catalyst; (**b**) EDS images and EDS-mapping of gold loaded biochar catalyst where BC1: 100 mg/L, BC2: 200 mg/L, BC3: 300 mg/L gold catalyst

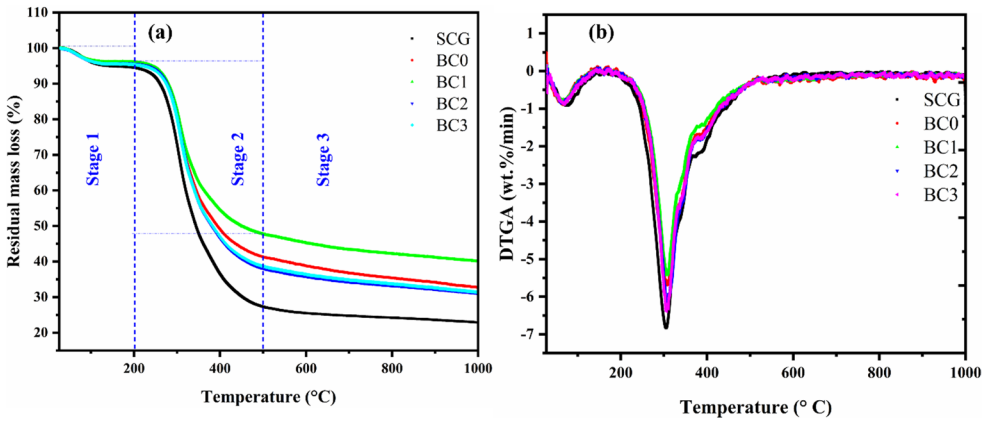

Fig. 4 (**a**) TGA and (**b**) DTGA of SCG with and without gold-loaded biochar catalysts BC0, BC1, BC2, and BC3

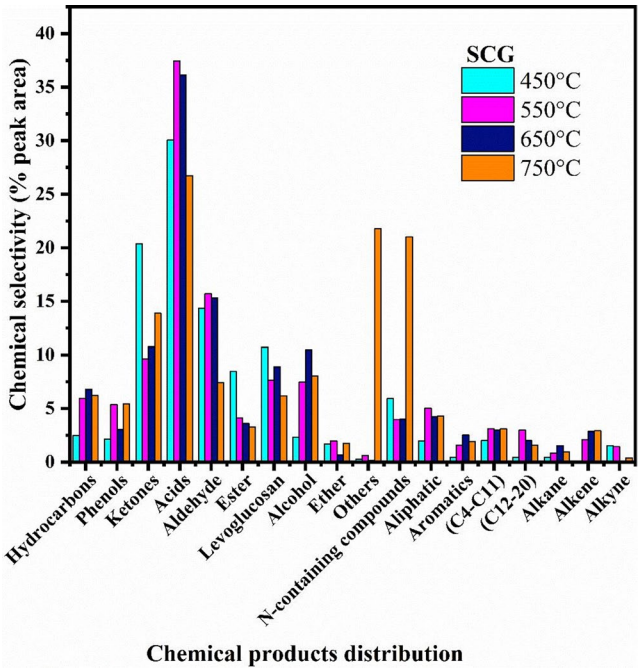

Fig. 5 Chemical products distribution of Spent coffee grounds at temperatures 450, 550, 650 and 750 °C

with various temperatures using BC3 catalysts as shown in Fig. 6 (d).

Notably, BC0 showed the highest amount of hydrocarbon production among all the catalysts, with the highest proportion of 11.11%. As the gold-loading onto the biochar increased, the selectivity of hydrocarbons increased at lower pyrolysis temperatures (450 and 550 °C). For example, at 450 °C, BC1 showed a hydrocarbon concentration of 1.27%, which increased to 2.05% for BC2 and 4.39% for BC3. However, at high pyrolysis temperature of 750 °C, the concentration of hydrocarbons consistently decreased with increasing the gold loading. For instance, BC1 achieved a hydrocarbon amount of 9.76%, whereas BC3 could only achieve 6.21% of hydrocarbons in the bio-oil. This decrease in catalyst activity can be attributed to the increased metal loading that can cause agglomeration of AuNPs on biochar surface, leading to quick deactivation of catalysts [48].

5.2.2 Effect of pyrolysis temperature on chemical product distribution

In catalytic reactions, reaction temperature is a critical element affecting the entire process. As shown in Fig. 7 depicts the results of studies performed at various pyrolysis temperatures (450, 550, 650, and 750 °C) of BC0, BC1, BC2, and BC3. The yields of phenols and aromatic hydrocarbons steadily climbed from below 4% to above 5.5% for phenols, as the temperature rose 450 to 750 °C, and from below 5% to above 9.9% for hydrocarbons. An additional temperature increase resulted in a slightly decrease in the selectivity of phenol at 750 °C, whereas hydrocarbons selectivity increased by approximately 10.5% for BC0, alongside an elevation in ketones and acids generation. This can be related to the cleavage of phenolic chains and the fracturing of the aromatic rings at increased temperatures [7]. Moreover, the formation of aromatics increased with the pyrolytic temperature for all the catalysts (irrespective of the comparative performance between all catalysts where non-catalytic pyrolysis showed the highest hydrocarbons formation of 11.11% at 750 °C.

Further, the highest conversion of alcohol occurred at 450 °C with BC1. For example, at approximately 480 °C, the methoxy groups in the ortho-position of the hydroxyl start to react [50]. The methoxy chemical group is changed to OH, CH_3, or H groups through different fragmentation reactions. Moreover, at 400 °C, the fragmentation of methoxy groups results in significant methanol production [50]. As shown in Fig. 7, levoglucosan was highest up to 25.5% at a temperature of 650 °C. Due to the fact that at temperatures exceeding 300 °C, the glycosidic bond exhibits significant reactivity, resulting in several simultaneous reactions [50]. Cellulose depolymerization occurs rapidly, producing about

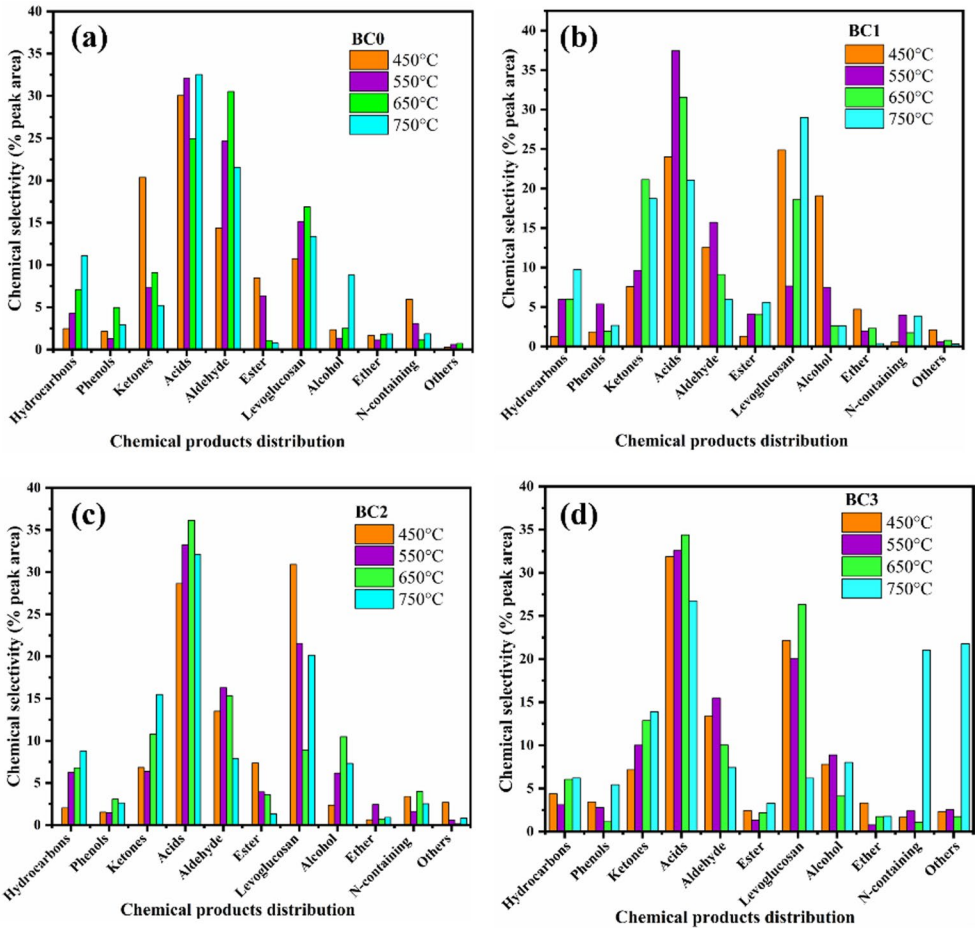

Fig. 6 Effect of gold-loaded biochar catalyst BC0, BC1, BC2 and BC3 on chemical products distribution at temperatures 450, 550, 650, and 750 °C

80% volatile chemicals, primarily condensable organic compounds. The depolymerization of cellulose results in a significant yield of levoglucosan [50].

The cellulose content in SCG can range from 30% to 40% [45]. For SCG, it has been investigated that cellulose breaks down at temperatures more than 180 °C and is fully depolymerized by 400 °C. This creates a wide range of organic compounds, such as aldehydes, furans, phenols, ketones, and acids [46]. The majority of the initial primary bonds between monomer chemical units have broken at temperatures exceeding 450 °C [50]. Therefore, the production of phenols (5.5%) is high at a temperature BC1-550 °C. For instance, around this temperature, the rupture of aromatic rings can occur, which produces the highest amount of phenols, and also the decomposition of SCG lignin is responsible for this conversion [50]. At the highest temperature (750 °C), the product distribution became more diversified. While acids remained significant, the formation of hydrocarbons and N-containing compounds became more pronounced, particularly for BC3. This suggests extensive secondary reactions such as cracking, cyclization, and condensation, which favor the formation of more thermodynamically stable compounds [7]. The reduction in oxygenated species (e.g., esters and ethers) at this temperature further confirms enhanced deoxygenation [7]. Overall, the results demonstrate that pyrolysis temperature greatly influences the distribution of chemical products, with low temperatures favoring oxygenated compounds such as acids, aldehydes, and levoglucosan, while higher temperatures promote secondary cracking, deoxygenation, and the formation hydrocarbons and N-containing species. Significant variations in chemical composition among BC1–BC3 further indicate that biochar modification with AuNPs alters thermal degradation pathways and product selectivity.

5.2.3 Effect of catalyst to feedstock ratio on chemical products distribution

The yields of chemical products were significantly influenced by the biochar catalyst-to-SCG ratio shown in Fig. 8. The number of hydrocarbons in the catalyst/feedstock ratio of 2:1 CP was higher than other ratios at a temperature of 650 °C for BC0 and 750 °C with BC1. A significant increase in hydrocarbons selectivity occurred when the catalyst-to-feedstock ratio shifted from 0:1 to 2:1 for BC1. However,

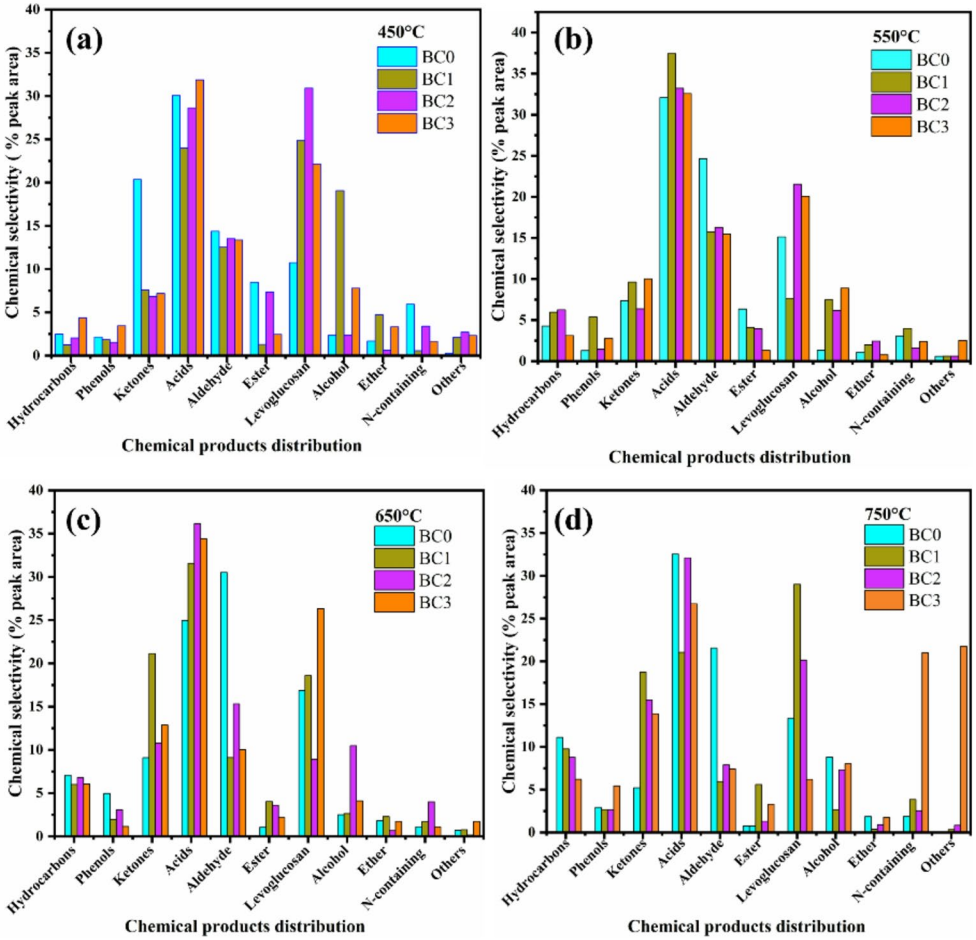

Fig. 7 Effect of pyrolysis temperature at 450, 550, 650, and 750 °C on chemical products distribution with different biochar catalysts BC0, BC1, BC2, and BC3

selectivity decreased with a subsequent change to a ratio of 1:1 for the BC3 catalyst.

The results indicated that the AuNPs-IBBC catalyst loading significantly influenced the composition of bio-oil and the production of hydrocarbons. The non-catalytic pyrolysis of SCG favored the formation of oxygenated compounds like ketones, acids, and hydrocarbons. In contrast, SCG catalytic pyrolysis with AuNPs-IBBC catalysts also influenced the generation of unique chemical compounds like levoglucosan.

It has been investigated that with a high SSA, the catalyst and volatiles can transfer more heat during thermal pyrolysis. Consequently, there are more sites for activity, which means the pyrolysis oil can undergo secondary pyrolysis more easily leading to the production of smaller molecules due to synergistic effect of C/F. The majority of minor oxygenated molecules (aldehydes, alcohols, ketones and esters) decreased with increased gold loading, demonstrating the deoxygenation capability of the AuNPs-IBBC catalyst BC1. The findings in this study can be compared with Douglas fir sawdust pellets biomass upgrading bio-oil [49]. For example, the hydrocarbons increased by 4.25% to 8.31% like Douglas fir biomass [49].

Overall, the catalyst-to-feedstock ratio strongly influences chemical product selectivity for all biochar catalysts (BC1–BC3). At lower catalyst loadings, primary oxygenated compounds such as acids, aldehydes, ketones, and levoglucosan dominated, indicating limited secondary conversions. Increasing the catalyst amount promoted cracking, dehydration, and rearrangement reactions, leading to reduced unstable species (e.g., esters and ethers) and redistribution of oxygenates. BC2 showed higher levoglucosan retention, suggesting milder catalytic activity, whereas BC3 facilitated stronger secondary transformations. These results indicate that excessive catalyst loading does not simply enhance conversion but redirects reaction pathways, emphasizing the importance of optimizing catalyst dosage.

5.2.4 Selectivity of hydrocarbon of all the catalyst (BC0, BC1, BC2 and BC3)

The catalytic pyrolysis with BC0 and BC1 produced total hydrocarbons constituted 11.18 and 9.76%, respectively, which was higher than BC2 (8.78%) and BC3 (6.20%). As illustrated in Fig. 9 the selectivity of aromatic hydrocarbons for SCG with BC1 was 5.5%. This result can be attributed

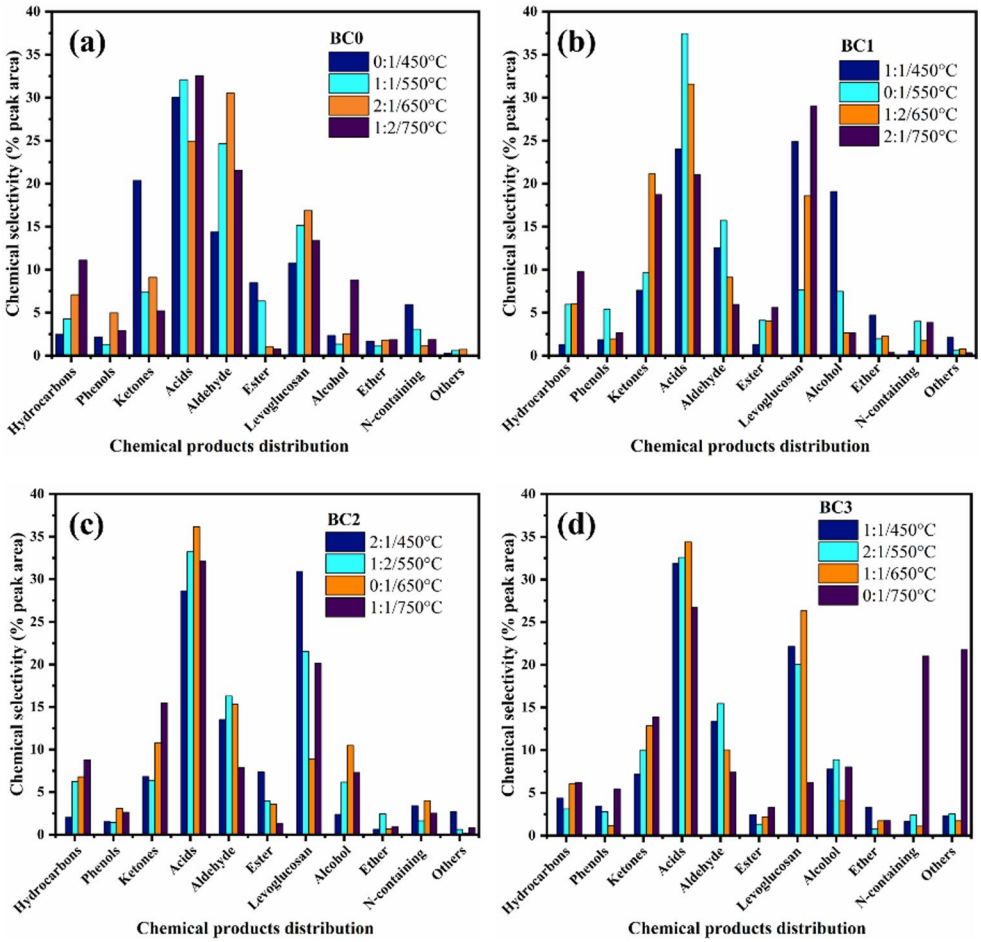

Fig. 8 Effect of catalyst to feedstock ratio on chemical products distribution at temperatures 450, 550, 650, and 750 °C of different biochar catalysts BC0, BC1, BC2, and BC3

to the increased gold concentration that facilitates electron supply for hydrocarbon radicals, subsequently, leading to further induced cracking reactions. For instance, the synergistic effect for aromatic hydrocarbons involved the replacement interaction of free radicals with phenols in the main pyrolytic oil, followed by a considerable increase in the yield of aromatics [21].

As for the gold catalysts, the BC1 catalyst favored C4–C11 hydrocarbons (with a selectivity of 6%), and it also produced 3.5% of the C5–C20 hydrocarbons. The reason can be that the gold nanoparticle-loaded biochar's porous structure as the total pore volume and pore diameter decreased compared to IBBC. Therefore, an optimal porous radius enhanced selectivity for aromatic hydrocarbons. Consequently, both BC2 and BC3 catalysts with low number of pores exhibited an aromatic yield around 2.9% only at 650 °C. The utilization of gold-loaded biochar supports in the CP of biomass resulted in similar aromatic hydrocarbons yield like the non-catalytic pyrolysis of SCG. To conclude, the presence of both mesopores and micropores in the biochar individually presented ideal active sites for the formation of aromatic hydrocarbons, while the presence of AuNPs played an important role to reduce some oxygenated compounds and influenced the formation of value-added chemicals like levoglucosan.

CP of SCG utilizing gold-loaded IBBC enhanced the concentration of C12−C20 compositions while decreasing the number of C4−C10 compositions. The rising levels of hydrocarbons may result from the degradation of aromatic polymer chains, the aromatization of alkenes and alkanes, or the condensation of monocyclic aromatics [51]. Alkanes, alkenes, and aromatics constitute significant constituents of bio-oils. Further, the addition of various catalysts enhances the reaction, consequently affecting the distribution of bio-oil to various levels.

6 Possible mechanism of the catalytic pyrolysis process of AuNPs-IBBC

As shown in Fig. 10, generally during SCG catalytic pyrolysis, cellulose and hemicellulose are converted into intermediate compounds mainly composed of sugars and furans, as well as anhydrous compounds, prior to reaching 450 °C temperature. Furthermore, depolymerization of SCG chemical compounds takes place within the temperature range

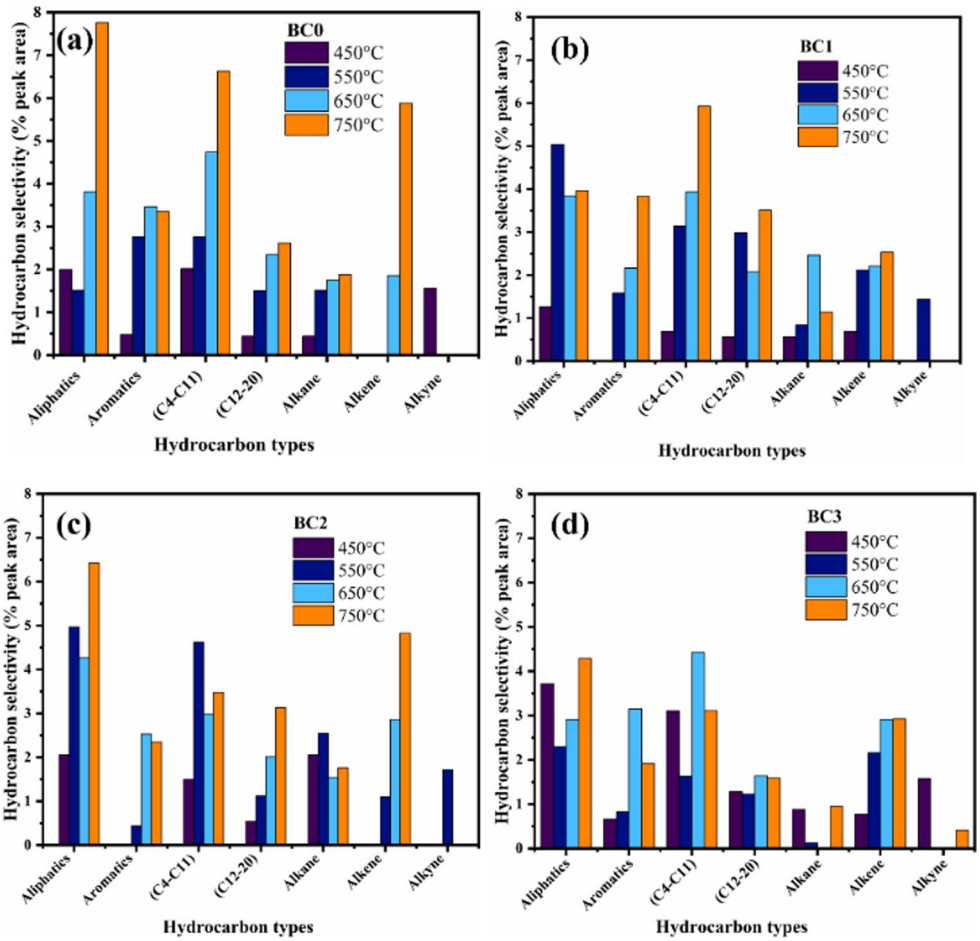

Fig. 9 Selectivity of hydrocarbon of different biochar catalysts BC0, BC1, BC2, and BC3 at temperatures 450, 550, 650, and 750 °C

of 200 to 500 °C. At these temperatures, the complicated macromolecular structure known as lignin undergoes depolymerization into smaller molecules such as aldehydes, phenols, and aromatic compounds [13]. Gold-loaded biochar catalysts also facilitate reactions such as cracking, decarboxylation, and decarbonylation and promote depolymerization prior to reaching 500 °C. The DTGA curve depicted in (Fig. 4b) shows that the maximum degradation occurs between 301.9 °C and 304.1 °C, whereas the thermal depolymerization of the SCG predominantly took place at 305 °C. Moreover, AuNPs-BC catalysts facilitate increased gas and coke production by promoting dehydrogenation and elevating the extent of ring-opening reactions within the temperature range of 500 to 1000 °C.

Further, the generation of phenols or hydrocarbons/ by AuNPs-IBBC demonstrates the significant deoxygenation effect of the biochar, involving decarboxylation, decarbonylation, and dehydration reactions. The acidic surface functional groups and SSA of biochar are likely the primary factors influencing its catalytic activity in aromatics and phenols production as shown in Fig. 2. It has been suggested that the glucose catalytic pyrolysis reaction pathway is responsible for the synthesis of aromatic hydrocarbons from aliphatic molecules [49], as depicted in Fig. 10.

Moreover, the IBBC biochar surface functional groups such as carboxylic acid groups facilitate the dehydration of sugars into furans, which subsequently conduct decarboxylation, oligomerization, and decarbonylation to yield aromatics. In the second step, aromatics are derived from lignin, which is primarily degraded into guaiacols and subsequently cleaved into phenols through the breaking of the phenol's O-CH_3 bond. For example, with the cleavage of the –OH group, phenols are converted to aromatics [49]. It has been also investigated that the existence of O-containing groups in biochar might facilitate the cleavage of the C-O linkage bonds in lignin [35]. In addition, O-R- groups, which are mainly –OH and –COOH, functioned like hydrogen givers, interacting with phenolic intermediates, which acted as hydrogen acceptors. In this process, however, the degradation of lignin is enhanced, whereas the degradation of hemicellulose and cellulose is prevented. Certain pyrolytic intermediates that possess functional groups such as O=C, –OH, and C-O showed enhanced catalytic activity [35]. Moreover, the rise in aromatics can be ascribed to

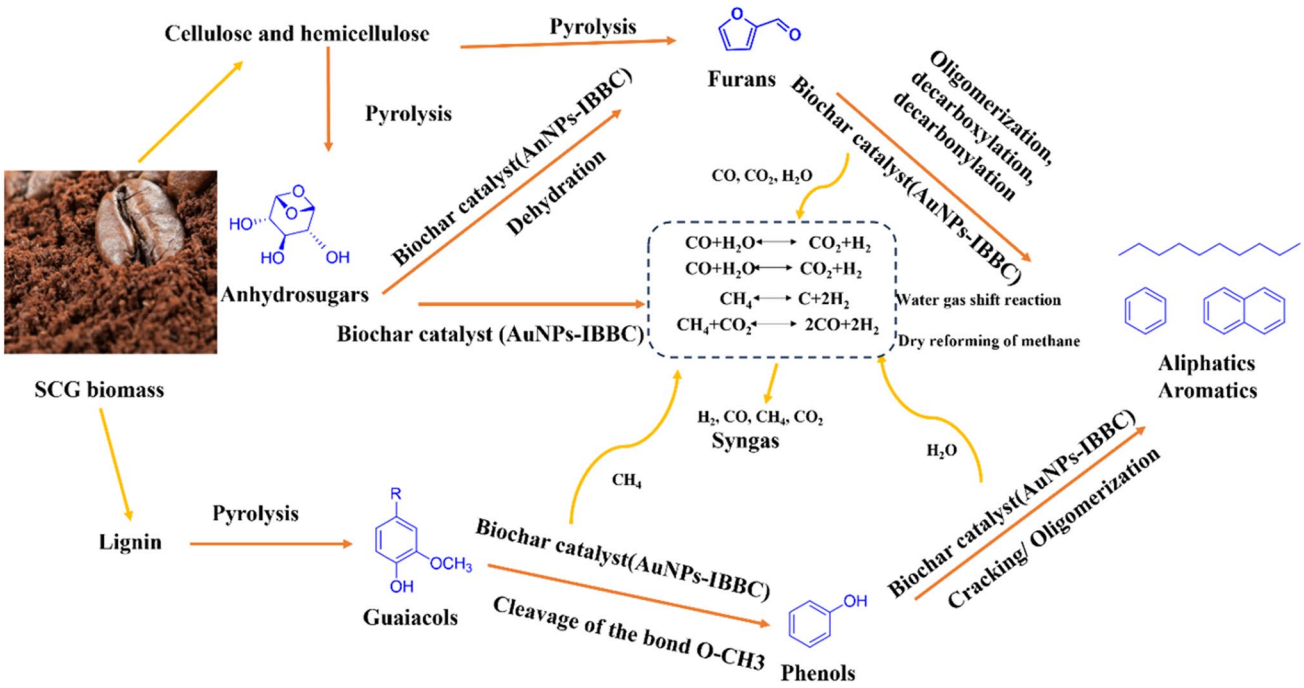

Fig. 10 Possible reactions occurred during catalytic pyrolysis of SCG with AuNPs-IBBC catalyst to produce hydrocarbons

the dehydration and condensation processes of ketones, together with the multi-step aromatization reactions of furfurals. The biochar catalyst, featuring carboxylic functional groups on its surface, facilitated the cracking and enhancement of bio-oils [49].

Regarding the enhancement of phenol content in bio-oil, the phenolic content of bio-oil demonstrates a positive correlation with the S_{BET} of BC1of catalysts. The findings demonstrate that the biochar catalysts predominantly have robust acid regions and include micro-mesoporous channels. The functional groups depicted in the FTIR of AuNPs-IBBC catalyst (BC1, BC2, and BC3) on carbon surfaces may exhibit acidic or basic properties, serving as active regions for diverse catalytic processes. O-containing surface functional groups exhibit mild acidity and provide enhanced catalytic reactions in acid-base processes and oxidation reactions [48].

7 Conclusion

This study demonstrates the effective use of IBBC as a catalyst support for upgrading spent coffee grounds (SCG) into valuable chemicals. Incorporating AuNPs onto the biochar surface produced a novel and cost-effective AuNPs-IBBC catalyst with enhanced structural properties and superior catalytic performance. The broadened pore size distribution and improved porosity of the biochar support facilitated the formation of aromatic hydrocarbons during catalytic pyrolysis. Compared with raw SCG pyrolysis, the AuNPs-IBBC catalyst significantly increased the yields of aliphatic and aromatic hydrocarbons as well as phenolic compounds. The BC1 catalyst showed the highest hydrocarbon (9.76%) and phenol (5.2%) production, with phenol formation reaching 5.5% at 550 °C. The catalyst also promoted a marked reduction in oxygenated and nitrogen-containing compounds in the bio-oil while increasing levoglucosan content, indicating effective deoxygenation and molecular upgrading. Overall, the results highlight a strong synergistic effect between IBBC and AuNPs, demonstrating that AuNPs-IBBC is a promising catalyst for efficient SCG valorization and the sustainable production of hydrocarbons and phenols.

Supplementary Information The online version contains supplementary material available at https://doi.org/10.1007/s13399-025-06936-4.

Authors' contributions Mahmuda Akter Mele: Methodology, data acquisition, data analysis, writing manuscript Ravinder Kumar: Writing, review and editing manuscript Ioan Sanislav: Review and editing manuscript Elsa Antunes: Conceptualization, supervision, review and editing manuscript.

Funding Open Access funding enabled and organized by CAUL and its Member Institutions. This research did not receive any funding.

Declarations

Competing interests All the authors have agreed to submit this manuscript to the journal of Biomass Conversion and Biorefinery. No actual or potential conflict of interest, including any financial, personal, or relationships with other people or organizations, could inappropriately influence the work.

References

1. Van Nguyen Q et al (2021) Co-pyrolysis of coffee-grounds and waste polystyrene foam: synergistic effect and product characteristics analysis. Fuel 292. https://doi.org/10.1016/j.fuel.2021.120375
2. Kanduri PK, Seethamraju S (2023) Effect of process mode on product yields and selectivity in the catalytic co-pyrolysis of peanut shells and polypropylene using spent fluid catalytic cracking (FCC) catalyst. Bioresour Technol Rep. https://doi.org/10.1016/j.biteb.2023.101478
3. Wang Y et al (2021) Review on the catalytic pyrolysis of waste oil for the production of renewable hydrocarbon fuels. Fuel 283. https://doi.org/10.1016/j.fuel.2020.119170
4. Kassa Dada T et al (2024) Enhanced catalytic activity of Sm/CeO2 to produce gasoline-range hydrocarbons from pyrolysis of spent coffee grounds. J Energy Inst 115. https://doi.org/10.1016/j.joei.2024.101663
5. Dada TK et al (2022) Catalytic co-pyrolysis of ironbark and waste cooking oil using X-strontium /Y-zeolite (X = Ni, Cu, Zn, Ag, and Fe). J Energy Inst 104:89–97. https://doi.org/10.1016/j.joei.2022.07.008
6. Dada TK et al (2021) A review on catalytic pyrolysis for high-quality bio-oil production from biomass. Biomass Convers Biorefinery 13(4):2595–2614. https://doi.org/10.1007/s13399-021-01391-3
7. Chen X et al (2024) Pyrolysis and catalytic upgrading of pine wood sawdust over modified Biochar catalyst in a tandem microreactor. J Anal Appl Pyrol 181. https://doi.org/10.1016/j.jaap.2024.106607
8. Gupta S, Patel P, Mondal P (2022) Catalytic pyrolysis using a Nickel-Functionalized chemically activated biochar catalyst: insight into process kinetics, products, and mechanism. ACS Sustain Chem Eng 10(18):5770–5780. https://doi.org/10.1021/acssuschemeng.1c08193
9. Liu S et al (2023) Catalytic pyrolysis of pine sawdust over activated carbon-supported Fe for phenol-rich bio-oil. J Anal Appl Pyrol 171. https://doi.org/10.1016/j.jaap.2023.105959
10. Pinard L et al (2024) Catalytic fast pyrolysis of biomass over hierarchical zeolites: comparison of Mordenite, Beta, and ZSM-5. Energy Fuels 38(15):14351–14364. https://doi.org/10.1021/acs.energyfuels.4c01188
11. Wu L et al (2022) Enhanced production of hydrocarbons from the catalytic pyrolysis of maize straw over hierarchical ZSM-11 zeolites. Appl Catal B 317. https://doi.org/10.1016/j.apcatb.2022.121775
12. Yang D et al (2024) Catalytic pyrolysis of lignin to aromatic hydrocarbons over Nb/Al oxide catalyst. Energy 302. https://doi.org/10.1016/j.energy.2024.131764
13. Peng H, Shahidi F (2023) Metabolic, toxicological, chemical, and commercial perspectives on esterification of dietary polyphenols: a review. Crit Rev Food Sci Nutr 1–40. https://doi.org/10.1080/10408398.2023.2185589
14. Zhang Y et al (2018) Renewable High-Purity Mono-Phenol production from catalytic Microwave-Induced pyrolysis of cellulose over Biomass-Derived activated carbon catalyst. ACS Sustain Chem Eng 6(4):5349–5357. https://doi.org/10.1021/acssuschemeng.8b00129
15. Nguyen VN et al (2024) Biochar-based catalysts derived from biomass waste: production, characterization, and application for liquid biofuel synthesis. Biofuels Bioprod Biorefin 18(2):594–616. https://doi.org/10.1002/bbb.2593
16. Balajii M, Niju S (2019) Biochar-derived heterogeneous catalysts for biodiesel production. Environ Chem Lett 17(4):1447–1469. https://doi.org/10.1007/s10311-019-00885-x
17. Behera B et al (2020) Algal biodiesel production with engineered Biochar as a heterogeneous solid acid catalyst. Bioresour Technol 310:123392. https://doi.org/10.1016/j.biortech.2020.123392
18. Cao X, Sun S, Sun R (2017) Application of biochar-based catalysts in biomass upgrading: a review. RSC Adv 7(77):48793–48805. https://doi.org/10.1039/C7RA09307A
19. Li S et al (2013) Biochar based solid acid catalyst hydrolyze biomass. J Environ Chem Eng 1(4):1174–1181. https://doi.org/10.1016/j.jece.2013.09.004
20. Chen W et al (2020) Bamboo wastes catalytic pyrolysis with N-doped Biochar catalyst for phenols products. Appl Energy 260. https://doi.org/10.1016/j.apenergy.2019.114242
21. Wang H et al (2018) Preparation of aromatic hydrocarbons from catalytic pyrolysis of microalgae/Palm Kernel Shell using PKS biochar-based catalysts. Energy Fuels 33(1):379–388. https://doi.org/10.1021/acs.energyfuels.8b03590
22. Fu J et al (2023) Co-circularity of spent coffee grounds and polyethylene via co-pyrolysis: Characteristics, kinetics, and products. Fuel 337. https://doi.org/10.1016/j.fuel.2022.127061
23. Vinod A et al (2020) Renewable and sustainable biobased materials: an assessment on biofibers, biofilms, biopolymers and biocomposites. J Clean Prod 258. https://doi.org/10.1016/j.jclepro.2020.120978
24. Annal UN et al (2024) Electrolytic biodiesel production from spent coffee grounds: optimization through response surface methodology and artificial neural network. J Taiwan Inst Chem Eng. https://doi.org/10.1016/j.jtice.2024.105697
25. Huang J et al (2024) Efficient bioethanol production from spent coffee grounds using liquid hot water pretreatment without detoxification. Fermentation 10(8). https://doi.org/10.3390/fermentation10080436
26. Shim H et al (2024) Enhancement of biohydrogen production and low coke formation by applying Ni/ZrxCe1-xO2 catalyst in steam gasification of spent coffee ground in monolithic reactor. Chem Eng J 484. https://doi.org/10.1016/j.cej.2024.149209
27. Islam MA et al (2022) Silver adsorption on biochar produced from spent coffee grounds: validation by kinetic and isothermal modelling. Biomass Convers Biorefin. https://doi.org/10.1007/s13399-022-03491-0

28. Cervera-Mata A et al (2022) Spent coffee grounds by-products and their influence on soil C-N dynamics. J Environ Manage 302(Pt B):114075. https://doi.org/10.1016/j.jenvman.2021.114075
29. Lee XJ et al (2021) Solid biofuel production from spent coffee ground wastes: process optimisation, characterisation and kinetic studies. Fuel 292. https://doi.org/10.1016/j.fuel.2021.120309
30. Kazmi WW et al (2024) Catalytic upgrading of the heavy fraction of waste coffee grounds pyrolysis bio-oil using supercritical ethanol as a hydrogen source to produce marine biofuel. Chem Eng Sci 287. https://doi.org/10.1016/j.ces.2024.119761
31. Lee HW et al (2020) Enhanced bioaromatics synthesis via catalytic co-pyrolysis of cellulose and spent coffee ground over microporous HZSM-5 and HY. Environ Res 184:109311. https://doi.org/10.1016/j.envres.2020.109311
32. Mele MA et al (2024) Investigation of gold adsorption by ironbark Biochar using response surface methodology and artificial neural network modelling. J Clean Prod 456. https://doi.org/10.1016/j.jclepro.2024.142317
33. Mer K et al (2024) Activation of sawdust Biochar with water and wastewater treatment residuals for sorption of perfluorooctanesulfonic acid in water. Chemosphere 358:142160. https://doi.org/10.1016/j.chemosphere.2024.142160
34. Qiu L et al (2024) Importance of oxygen-containing functionalities and pore structures of Biochar in catalyzing pyrolysis of homologous Poplar. Chin J Chem Eng 65:200–211. https://doi.org/10.1016/j.cjche.2023.09.002
35. Yang H et al (2020) Role of porous structure and active O-containing groups of activated Biochar catalyst during biomass catalytic pyrolysis. Energy 210. https://doi.org/10.1016/j.energy.2020.118646
36. Qiu Z et al (2018) Biochar-based carbons with hierarchical micro-meso-macro porosity for high rate and long cycle life supercapacitors. J Power Sources 376:82–90. https://doi.org/10.1016/j.jpowsour.2017.11.077
37. Ganash A, Alshammari S, Ganash E (2022) Development of a novel electrochemical sensor based on gold Nanoparticle-Modified Carbon-Paste electrode for the detection of congo red dye. Molecules 28(1). https://doi.org/10.3390/molecules28010019
38. Mo Z et al (2021) Efficient removal of Cd(II) from aqueous environment by potassium permanganate-modified eucalyptus biochar. Biomass Convers Biorefin. https://doi.org/10.1007/s13399-021-02079-4
39. Hossain MK et al (2011) Influence of pyrolysis temperature on production and nutrient properties of wastewater sludge Biochar. J Environ Manage 92(1):223–228. https://doi.org/10.1016/j.jenvman.2010.09.008
40. Lu H et al (2013) Characterization of sewage sludge-derived biochars from different feedstocks and pyrolysis temperatures. J Anal Appl Pyrol 102:137–143. https://doi.org/10.1016/j.jaap.2013.03.004
41. Zhang X, Zhang L, Li A (2018) Eucalyptus sawdust derived biochar generated by combining the hydrothermal carbonization and low concentration KOH modification for hexavalent chromium removal. J Environ Manage 206:989–998. https://doi.org/10.1016/j.jenvman.2017.11.079
42. Singh R et al (2021) High surface area Eucalyptus wood Biochar for the removal of phenol from petroleum refinery wastewater. Environ Challenges 5. https://doi.org/10.1016/j.envc.2021.100353
43. Yusuff AS et al (2022) ZnCl2-modified Eucalyptus bark Biochar as adsorbent: preparation, characterization and its application in adsorption of Cr(VI) from aqueous solutions. S Afr J Chem Eng 42:138–145. https://doi.org/10.1016/j.sajce.2022.08.002
44. Yang X et al (2019) Unveiling the pyrolysis mechanisms of Hemicellulose: experimental and theoretical studies. Energy Fuels 33(5):4352–4360. https://doi.org/10.1021/acs.energyfuels.9b00482
45. Bomfim AS et al (2022) Spent coffee grounds characterization and reuse in composting and soil amendment. Waste 1(1):2–20. https://doi.org/10.3390/waste1010002
46. Ansari KB et al (2019) Fast pyrolysis of cellulose, Hemicellulose, and Lignin: effect of operating temperature on bio-oil yield and composition and insights into the intrinsic pyrolysis chemistry. Ind Eng Chem Res 58(35):15838–15852. https://doi.org/10.1021/acs.iecr.9b00920
47. Kelkar S et al (2015) Pyrolysis of spent coffee grounds using a screw-conveyor reactor. Fuel Process Technol 137:170–178. https://doi.org/10.1016/j.fuproc.2015.04.006
48. Zou R et al (2022) Biochar: from by-products of agro-industrial lignocellulosic waste to tailored carbon-based catalysts for biomass thermochemical conversions. Chem Eng J 441. https://doi.org/10.1016/j.cej.2022.135972
49. Ren S et al (2014) Hydrocarbon and hydrogen-rich Syngas production by biomass catalytic pyrolysis and bio-oil upgrading over Biochar catalysts. RSC Adv 4(21):10731–10737. https://doi.org/10.1039/c4ra00122b
50. Collard F-X, Blin J (2014) A review on pyrolysis of biomass constituents: mechanisms and composition of the products obtained from the conversion of cellulose, hemicelluloses and lignin. Renew Sustain Energy Rev 38:594–608. https://doi.org/10.1016/j.rser.2014.06.013
51. Sun K et al (2018) Producing Aromatic-Enriched oil from mixed plastics using activated Biochar as catalyst. Energy Fuels 32(4):5471–5479. https://doi.org/10.1021/acs.energyfuels.7b03710